



Published in final edited form as:

*Cell Tissue Res.* 2012 August ; 349(2): 505–515. doi:10.1007/s00441-012-1423-7.

## Defining Essential Stem Cell Characteristics in Adipose-Derived Stromal Cells Extracted from Distinct Anatomical Sites

Patrick C. Sachs<sup>1</sup>, Michael P. Francis<sup>2</sup>, Min Zhao<sup>2</sup>, Jenni Brumelle<sup>2</sup>, Raj R. Rao<sup>1,3,5</sup>, Lynne W. Elmore<sup>2,5,\*</sup>, and Shawn E. Holt<sup>1,2,4,5,6,\*</sup>

<sup>1</sup>Department of Human and Molecular Genetics, Medical College of Virginia Campus, Virginia Commonwealth University, 1101 E. Marshall St., Richmond, VA 23298-0662

<sup>2</sup>Department of Pathology, Medical College of Virginia Campus, Virginia Commonwealth University, 1101 E. Marshall St., Richmond, VA 23298-0662

<sup>3</sup>Chemical and Life Science Engineering, Medical College of Virginia Campus, Virginia Commonwealth University, 1101 E. Marshall St., Richmond, VA 23298-0662

<sup>4</sup>Department of Pharmacology and Toxicology, Medical College of Virginia Campus, Virginia Commonwealth University, 1101 E. Marshall St., Richmond, VA 23298-0662

<sup>5</sup>Massey Cancer Center; Medical College of Virginia Campus, Virginia Commonwealth University, 1101 E. Marshall St., Richmond, VA 23298-0662

<sup>6</sup>Department of Biology, Virginia State University, Petersburg, VA 23806

### Abstract

The discovery of adipose-derived stromal cells (ASCs) has created many opportunities for the development of patient-specific cell-based replacement therapies. We have isolated multiple cell strains of ASCs from various anatomical sites (abdomen, arms/legs, breast, buttocks), indicating wide-spread distribution of ASCs throughout the body. Unfortunately, there exists a general lack of agreement in the literature as to their “stem cell” characteristics. We find that telomerase activity and expression of its catalytic subunit in ASCs are both below the levels of detection, independent of age and culturing conditions. ASCs also undergo telomere attrition and eventually senesce, while maintaining a stable karyotype without the development of spontaneous tumor-associated abnormalities. Using a set of cell surface markers that have been promoted to identify ASCs, we find that they failed to distinguish ASCs from normal fibroblasts, as both are positive for CD29, CD73, and CD105 and negative for CD14, CD31, and CD45. All of the ASC isolates are multipotent, capable of differentiating into osteocytes, chondrocytes, and adipocytes, while fibroblasts show no differentiation potential. Our ASC strains also show elevated expression of genes associated with pluripotent cells, Oct-4, SOX2, and NANOG when compared to fibroblasts and bone marrow-derived mesenchymal stem cells (BM-MSCs), although the levels were lower than induced pluripotent stem cells (iPS). Together, our data suggest that while the cell surface profile of ASCs does not distinguish them from normal fibroblasts, their differentiation capacity and the expression of genes closely linked to pluripotency clearly define ASCs as multipotent stem cells, regardless of tissue isolation location.

\*Address for correspondence and reprints: Lynne W. Elmore, Ph.D., Department of Pathology, Medical College of Virginia at VCU, 1101 E. Marshall St., Richmond, Virginia 23298-0662, Ph: (804) 628-0256, lemores@mcvhvcu.edu. Shawn E. Holt, Ph.D., Department of Biology, Virginia State University, 1 Hayden Dr., Petersburg, Virginia 23806, Ph: (804) 514-5839, sholt@vsu.edu.

#### Author Disclosure

All authors agree to the format and content of the manuscript, and none have any commercial affiliations or associations that would contemplate a conflict of interest for the data presented.

## Keywords

ASC; iPS; Pluripotent; Stem Cell; Telomere; Telomerase

---

## Introduction

The utility of adult stem cells presents a unique opportunity for the development of low cost, low risk methods to treat human disease using patient-specific cells. Current techniques employ a generally low yield isolation protocol for bone marrow-derived mesenchymal stem cells (BM-MSCs) from the iliac crest of the pelvis (1), which is an invasive and painful procedure. More recently, a cell type similar to BM-MSCs was discovered residing in fat tissue removed during elective lipoaspiration surgeries. These cells, appropriately named adipose-derived stromal cells (ASCs), are isolated with much higher efficiency relative to the BM-MSC isolations, have a greater expansion capacity, and appear to differentiate efficiently into the same cell lineages as BM-MSCs (2). Following their discovery, the stem cell-like qualities of ASCs came under scrutiny as their identity and characteristics were still being determined. Many groups have attempted to define a specific set of cell surface markers to purify ASCs from the complex mix of cells in the stromal vascular fraction (SVF) isolated from lipoaspirate. A variety of combinations have been attempted with varying results (1–13), but a general lack of agreement exists as to which of these factors are the most relevant.

In an effort to distinguish ASCs from normal fibroblasts, many studies have attempted to identify unique ASC properties, including their resident niche, their stability in culture, and their gene expression profile (1,8). Recently, a report showing that some ASCs undergo spontaneous transformation and/or aneuploidy with continuous culture was retracted based on data indicating tumor cell cross-contamination (14), which was not overly surprising given that the vast majority of studies show no such transformation potential (13,15,16). There has also been interest defining a set of genes, such as Oct-4 and hTERT, which would suggest these ASCs are more embryonic-like than the morphologically similar fibroblast cells. It has been reported that ASCs express hTERT and some reports show expression of genes associated with pluripotency such as Oct-4 (8,13,16,17). The indication that ASCs express markers of pluripotency suggests that these cells have characteristics similar to embryonic stem cells (ESCs) while being able to maintain the mesenchymal state of normal fibroblasts.

Using multiple ASC isolations from various tissue sites within the human body, we demonstrate that the expression of a widely used set of cell surface markers fails to distinguish ASCs from fibroblasts, suggesting that identifying adult stem cells likely will not be based on their cell surface characteristics. In order to more accurately define the stemness of our ASC cultures, we find that the differentiation capacity and the expression profile of certain pluripotent genes provide evidence of their multipotency and functional stem cell qualities. Thus, their ability to differentiate into mesenchymal cell types (fat, bone, cartilage) and their elevated expression of ESC-related transcription factors (Oct-4, SOX2, NANOG) functionally distinguish ASCs as mesenchymal stem cells, independent of the anatomical site of harvest (abdomen, arms/legs, breast, or buttocks).

## Materials and Methods

### ASC isolation

Isolation was carried out as described previously (2) except where noted. Freshly harvested fat was obtained and immediately subjected to isolation. All patient samples were treated as

medical waste and were therefore not subjected to Institutional Review Board approval. Any separated oil was removed from the top of the lipoaspirate followed by the removal of the saline/blood fraction. For the ASC 12s strain, we modified the protocol by removing the saline fraction into a separate conical tube in order to pellet the cells as previously described (18). The fraction of mononuclear cells was then resuspended in 25ml DMEM/F12 supplemented with 50% FBS, 1% antibiotic/antimycotic (ABAM) (Invitrogen), and 10ng/ml EGF, followed by incubation overnight to select for adherence. The remaining floating cells were aspirated off the following day, and the adherent cells were washed to remove any remaining red blood cells or fat lobules. All ASC cell strains were isolated from different individuals as noted by the increasing numerical value, i.e. ASC 1, 4, 5, 6, 8, 9, 12s. ASC isolations were from various sites in the body with ASC 1, 4, 8 from the abdomen, ASC 9 from the legs and arms, and ASC 12s from the buttocks (ASC 5 and ASC 6 tissue sites were not noted), as well as bASC 1, 2, 3, 4 from breast tissue from reduction mammoplasty.

### Cell Culture

All ASC cell strains were maintained in DMEM low glucose supplemented with 10% FBS, 1% antibiotic/antimycotic (ABAM, Invitrogen), and 10ng/ml EGF in 5% CO<sub>2</sub> at 37°C. All versions of BJ fibroblasts cells (CRL-2522, ATCC, Manassas, VA), post natal foreskin fibroblasts, were cultured in DMEM high glucose supplemented with 10% cosmic calf serum (Thermo Scientific, Waltham, MA), 3% Media 199 (Invitrogen, Carlsbad, CA), and 1% ABAM. Stable BJ-hTERT cells were made by retroviral infection of the catalytic subunit gene (hTERT) of telomerase and used as a positive control for telomere length assays (19,20). BJ-GFP, ASC 8-GFP and ASC 8-hTERT cells were established by infection of the green fluorescent protein (GFP) gene and the hTERT gene using Adenoviral-mediated infection, serving as a negative (GFP cells) and a positive (hTERT) control for telomerase assays (19).

Induced pluripotent stem (iPS) cells (from Dr. James Thomson, University of Wisconsin) and embryonic stem cells (ESCs; BG01V clone, ATCC) were maintained on mytomycin C (Sigma) inactivated mouse embryonic fibroblasts monolayer in knock out replacement media (KoSR) containing DMEM/F12, 20% KoSR (Invitrogen), 1% penicillin/streptomycin (Invitrogen), 1% non-essential amino acids (Invitrogen), 0.1mM  $\beta$ -mercaptoethanol (Sigma), and 4ng/ml basic Fibroblast Growth Factor (bFGF) (Invitrogen). HL-60 promyelocytic leukemia cells (CCL-240, ATCC) were grown in suspension in DMEM with 10% serum and 1% ABAM and were used as positive controls for telomerase activity assays (19,20).

### Karyotypic Analysis

The chromosomes from cell strains ASC 8, ASC 9, and ASC 12s were analyzed using GTG-banding. Each cell line was harvested and slides were prepared according to standard procedures (21). Briefly, actively dividing cells were blocked in metaphase with 0.1g/ml of Colcemid for 2–4 hours. After a 10min incubation in a 0.075M KCl hypotonic solution, the cells were fixed by serial washes in a methanol/glacial acetic acid solution (3:1). GTG-banding was performed using standard procedures (22). Representative images were captured using a Cytovision image analysis system (Applied Imaging, Santa Clara, CA) and scored as before (20).

### Adipocyte Differentiation

Cells were plated, grown to 100% confluence, and incubated in adipogenic media containing DMEM low glucose, 1% FBS, 0.5mM isobutyl-methylxanthine (Sigma), 1 $\mu$ M dexamethasone (Sigma), 10 $\mu$ M insulin (Sigma), 200 $\mu$ M indomethacin (Sigma), and 1% ABAM. The plates were maintained for 2 weeks until lipid droplets formed. The cells were

then washed and fixed using 4% paraformaldehyde and stained with Oil Red O (Sigma), which specifically stains lipids. Whole field light microscopy images were captured at 10x magnification.

### **Osteocyte Differentiation**

Cells were plated and grown to approximately 75% confluence, and then osteogenic differentiation media was added. The differentiation media consisted of DMEM high glucose, 1% FBS, 0.01 $\mu$ M 1,25-dihydroxyvitamin D3 (Sigma), 50 $\mu$ M ascorbate-2-phosphate (Sigma), 10mM  $\beta$ -glycerophosphate (Sigma), and 1% ABAM. The cells were cultured for 2 weeks until significant calcium deposits were observed. The cells were then washed and fixed using 4% paraformaldehyde solution and stained using Alizaran Red S (Sigma), which specifically stains calcified deposits in the extracellular matrix. Whole field light microscopy images were captured at 10x magnification.

### **Chondrocyte Differentiation**

Cells were collected and pelleted at 300xg in a 2ml V bottomed tube at  $2 \times 10^5$  cells per pellet. These tubes were placed in the incubator at 37°C in 5% CO<sub>2</sub> in chondrogenic differentiation media containing DMEM low glucose, 1% FBS, 6.25 $\mu$ g/ml insulin, 10ng/ml recombinant TGF3 (R&D Systems, Minneapolis, MN), 50nM ascorbate-2-phosphate, and 1% ABAM. After 1 week, the pellets were transferred to a 10cm<sup>2</sup> dish and cultured in the same media formulation for another 2 weeks. The pellets were then removed, and the remaining cells on the plate were fixed in 4% paraformaldehyde and stained with Safranin O (Sigma), which specifically detects glycosaminoglycans (GAG) proteins present in high concentrations in chondrocyte extracellular matrix.

### **Telomeric Repeat Amplification Protocol (TRAP)**

For the detection of telomerase activity, the TRAPeze kit (Millipore, Billerica, MA) protocol was followed as before (19,20). Briefly, 100,000 cells were lysed in 200 $\mu$ l of CHAPS lysis buffer with protease inhibitors to achieve a concentration of 500 cells/ $\mu$ l. Subsequent lysates were either used immediately or stored at -80°C until analyzed. The TRAP assay was carried out using  $\gamma^{32}$ P-ATP labeled TS-primer and 1000 cells (2 $\mu$ l) per sample, followed by PCR amplification. Telomerase-extended products were visualized by electrophoresis on a 10% polyacrylamide gel, followed by a brief fixation and exposure to a phosphorimager screen overnight. The subsequent radiographic image was captured and quantified as before (20), using a Molecular Dynamics phosphorimager and ImageQuant software (Molecular Dynamics, Sunnyvale CA).

### **Terminal Restriction Fragment Analysis (TRF)**

Genomic DNA from  $2 \times 10^7$  cells was isolated using the Qiagen genomic extraction kit, following the provided protocol (Qiagen, Valencia, CA). A telomere specific oligonucleotide G-rich probe (5'-TTAGGGTTAGGGTTAGGG-3') was labeled using  $\gamma^{32}$ P-ATP for use in the TRF assay, as before (20). Following in-gel hybridization and washing, the gel was exposed to a phosphorimager cassette and imaged using a phosphorimager and analyzed using ImageQuant software (Molecular Dynamics). Total area under the curve was calculated following area densitometry and the mean value is shown as before (19,20).

### **Flow Cytometry**

500,000 cells/sample were centrifuged at 1000xg for 1min at 4°C, resuspended in 75 $\mu$ l of FACS buffer (PBS, 2% FBS), and incubated on ice for 10 minutes. Cell were immunolabeled with 13 $\mu$ g/ $\mu$ l of the respective primary antibody (CD14, CD29, CD31, CD34, CD45, CD73, or CD105) (Millipore) for 30mins at 4°C with rotation, followed by

centrifugation and 3 washes with FACS buffer. Secondary antibody (Alexa 488 anti-mouse, Molecular Probes) was added at a dilution of 1:400 and incubated in the dark at 4°C with rotation for 30min. After washing, the resulting pellet was resuspended in 500µl PBS and filtered through a 35µm nylon mesh to remove aggregated cells. Cell suspensions were kept on ice until cytometric analysis, which was performed using a Coulter Epics XL-MCL (Beckman Coulter, Brea, CA).

### Gel-based RT-PCR and qRT-PCR

Total RNA was extracted using TRIzol (Invitrogen) reagent following the manufacturer's protocol as before (20). RNA purity and concentration was analyzed using a Nanodrop 1000 UV/Spectrophotometer (Thermo Scientific, Waltham, MA). RT-PCR was then carried out using the RETROscript kit protocol (Ambion, Austin, TX), as before (19,20). The PCR conditions were 94°C for 2 minutes, 30 cycles of 94°C for 30 seconds, 55°C for 30 seconds, 72°C for 1 minute, and 72°C for 5 minutes. Primers used were as follows: Oct-4 Fwd 5'-CAGTGCCCGAAACCCACAC-3', Rev 5'-GGAGACCCAGCAGCCTCAAA-3'; SOX2 Fwd 5'-TACCTCTCCTCCCACTCCA-3', Rev 5'-GGTAGTGCTGGGACATGTGA-3'; NANOG Fwd 5' TTTGGAAGCTGCTGGGGAAG 3', Rev 5' GATGGGAGGAGGGGAGAGGA 3'; hTERT Fwd 5'-CGGAAGAGTGTCTGGAGCAA-3', Rev 5'-GGATGAAGCGGAGTCTGGA-3'. The resulting PCR products were visualized after electrophoresis on a 1.5% agarose gel and staining with ethidium bromide.

For qRT-PCR, the resulting cDNA was then used to create a standard curve for optimized cDNA amplification and primer dissociation of each primer set (above) using the SYBR-greener qRT-PCR Supermix kit (Invitrogen). Primers used for the genes of interest were as above. Relative quantitative polymerase chain reaction (qRT-PCR) was carried out using an Applied Bioscience 7900HT instrument. The resulting data was analyzed using the 2- $\Delta\Delta C_t$  method with ABI SDS 2.2.2 software (Applied Bioscience) where ribosomal 18S (Ambion, Austin, TX) gene served as the endogenous control, and baseline gene expression was set to signal levels from normal BJ fibroblasts. All data shown was significant ( $p < 0.05$ ) versus BJ cells; analysis was done using a student T-test.

## Results

### ASCs can be isolated from many sources, have normal growth and are karyotypically stable

Our ASC isolations were similar to previous studies showing an abundance of adherent cells with a 100-fold increase in viable cells when compared to those isolated from bone marrow aspiration (1,2,13). Because prior studies suggested that ASCs reside in a niche located in the perivascularity of capillaries and arterioles (8), we hypothesized that the blood/saline fraction of lipoaspiration procedures might contain a subset of ASCs, released in part due to the disruptive nature of the lipoaspiration procedure. Our more recent isolations used a modification of the existing extensive 8–10 hour protocol reduced to a simple 30 minute procedure (18), resulting in the successful isolation of ASCs using this rapid protocol (ASC 12s). We assumed that these cells reside in the capillary beds interspersed throughout fatty deposits, making it possible to obtain ASCs from many other localities in the body. It is also important to note that all of the isolated ASCs were from women undergoing liposuction, abdominoplasty, or breast reduction. In fact, we successfully isolated ASCs from fat tissue from multiple patients throughout the abdomen (ASC 1, 4, 8), legs and arms (ASC 9), buttocks (ASC 12s), and four successful isolations from four individual breast reduction mammoplasties (bASC 1–4).

Although only the data for ASC 8, ASC 9, and ASC 12s is shown, we observed a comparable doubling time (24–50 hours) with an appropriate proliferative lifespan, ranging from 30–50 population doublings (PDs), for all of our ASC cell strains (Table 1), consistent with other reports (1–13). Based on patient age presented in Table 1, there appears to be an association of donor age at harvest with overall lifespan of ASCs in 3 of our 14 lines. Additional lifespan determinations were done with other lines, showing that bASC 2 (donor age 16), bASC 3 (donor age 45), and bASC 4 (donor age 32) had lifespans of ~25 PDs, ~40 PDs, and ~28 PDs, respectively (data not shown), suggesting no apparent correlation between patient age at isolation and ASC lifespan. An examination of karyotypic stability with continued passage showed that our ASCs were karyotypically stable at both early and late population doublings (PDs) (Table 1) with no evidence of karyotypic changes associated with transformation to a cancer-like state.

### **ASCs lack telomerase and show telomere erosion with serial passaging**

Due to the finite lifespan of our ASCs following continued passage (Table 1), we wanted to determine the potential mechanism for proliferative lifespan limits. Previous ASC studies have shown the presence of the catalytic component of telomerase, hTERT, (8,23) or telomerase activity (1,24), while others report a lack of telomerase expression in ASCs (4,25) and that introduction of exogenous hTERT in telomerase-negative ASCs results in elevated telomerase activity (26,27). To evaluate our cells for telomerase activity, we used a variety of culture conditions: day 0 cultures, low population doubling (PD 2) cells, actively dividing ASCs, and ASCs grown in ESC media. ASCs isolated from all tissue locations exhibited a complete lack of telomerase activity in all conditions tested (Figure 1a). Additional reports indicate elevated telomerase expression in BM-MSCs upon culturing after serum deprivation (17,28), yet repeated attempts to stimulate our ASC cultures after serum starvation failed to show any telomerase activation even though the cells were actively dividing (not shown). In addition, we examined the levels of hTERT mRNA using standard, gel-based RT-PCR (Figure 1b) and found no detectable hTERT expression in any of our cultures. Additional attempts at detecting hTERT using real-time RT-PCR also suggested levels of hTERT expression below the limits of detection (data not shown). Given the complete lack of detectable telomerase, we expected gradual telomere erosion in our ASCs and examined global telomere lengths with continued culturing (Figure 1c). As anticipated, we found that overall telomere lengths decrease in ASCs with successive PD in samples from the various tissue types, correlating the progressive loss of proliferative capacity to gradual telomere shortening (Figure 1c). In addition, our ASCs at high PD exhibited widespread senescence-associated  $\beta$ -galactosidase (SA- $\beta$ -gal) (20), indicating the induction of senescence as a consequence of telomere erosion, an example of which, compared to young ASCs (Figure 1d), is shown in Figure 1e.

### **ASCs immunophenotype is indistinguishable from normal fibroblasts**

To clarify the combination of markers most appropriate for classifying our ASCs as stem cells, we tested a panel of antibodies most commonly reported in recent literature (1–13). While there are many conflicting reports, some commonly used cell surface markers do exist (Table 2). We focused on a consensus set of markers derived from current literature (Table 2), most of which were promoted by commercial sources as adult stem cell markers. The positive markers included: CD29 (stains a diverse number of cells including endothelial cells, monocytes, and platelets), CD73 (found on epithelium, endothelial, and some mature lymphocytes), CD105 (a marker of endothelium and perhaps some stem/progenitors), and the more controversial marker, CD34, which is primarily found on hematopoietic stem cells. For negative cell surface markers, we used a panel of antibodies generally accepted as negative for mesenchymal cells including: CD45 (a general marker of leukocyte presence),

CD31 (a marker of endothelial cells), and CD14 (used to distinguish cells from macrophages/monocytes).

We first tested the iPS line derived from BJ fibroblasts to determine if these cells were similar to our stem cells and found a complete lack of expression for all surface markers tested (data not shown). Our ASC strains from all tissue isolation sites consistently stained positive for CD29, CD73, CD105 with undetectable immunoreactivity for CD45, CD31, and CD14 (Table 2). However, we found a small population of cells in the ASC cultures that express CD34, whereas the CD34 marker was completely absent from BJ fibroblasts and iPS cells. Using careful analysis to show individual cell fluorescence more clearly, the expression of CD34 was low enough (<8%) that ASCs could easily be called negative if using the traditional examination methods; thus, we classified our ASCs as CD34<sup>low</sup> (Table 2). Other than the very low expression of CD34 within the ASC populations, BJ fibroblasts showed an indistinguishable cell surface pattern relative to our ASC strains, suggesting that the immunophenotype of ASCs does not classify them as stem cells. As a positive control for staining with the antibodies for CD14, CD31, and CD45, we used HL-60 cells subjected to differentiation after Vitamin D exposure (not shown).

### ASCs have high multipotency

In an effort to distinguish our ASCs from normal fibroblasts, we determined their multipotent capabilities by differentiating cells down multiple mesenchymal lineages as reported previously (1–13). First, we tested their ability to differentiate into their source cell type, adipocytes, using an adipogenic cocktail media with BM-MSCs serving as the positive control. Whether isolated from the saline fraction, abdomen, arms/legs, breasts, or buttocks, all ASCs successfully differentiated into adipocytes, as did the BM-MSCs (Figure 2a). There was no differentiation observed in BJ fibroblast controls (Figure 2a) or from ASCs and BM-MSCs maintained at confluence for 2–3 weeks in regular growth media without the adipogenic cocktail (Control Media) (Figure 2a). Successful differentiation into adipocytes was initially characterized morphologically by the formation of round lipid droplets within the cell, which was then confirmed by staining with the lipid and neutral triglyceride-specific stain, Oil Red O. We have confirmed the fat differentiation by finding a substantial increase in the expression levels of the adipogenic markers PPAR $\gamma$  (peroxisome proliferator activated receptor) and lipoprotein lipase (data not shown).

To determine ASCs' ability to differentiate into bone, we subjected cells to a media cocktail containing elements to specifically cause osteogenic differentiation. Morphologically, the cells began to group together and form “bone nodules”, a characteristic of osteogenesis *in vitro*, which was confirmed by staining with Alizaran Red S to visualize the calcification in the surrounding extracellular matrix (Figure 2b). All ASCs from the various tissues and BM-MSCs, but not BJ fibroblasts or cells grown in normal growth media without the osteogenic cocktail (Control Media), differentiated along an osteogenic lineage in induction media (Figure 2b). To further confirm bone differentiation, elevated levels of both alkaline phosphatase and osterix were observed by qRT-PCR (data not shown).

To classify our ASCs as multipotent, we tested their capacity to differentiate down a chondrogenic pathway by maintaining the cells in a chondrogenic differentiation cocktail for 30 days. Again, all ASC cell types and the BM-MSCs successfully differentiated into a solid chondrogenic micromass pellet that stained positively for the GAG protein-specific Safranin O, which was absent in BJ fibroblasts (Figure 2c). In our hands, normal BJ fibroblasts failed to differentiate down any of the three mesenchymal lineages tested, despite a report indicating their ability to differentiate into chondrocytes (5). The BM-MSCs, while variable in their differentiation capacity, were capable of differentiating into all 3 of the mesenchymal lineages tested. Importantly, our rapid isolation ASC strains (ASC 12s is

shown), as well as all ASCs from the various tissue types, show the ability to differentiate into mesenchymal lineages, including bone, fat, and cartilage (Figure 2) (18).

### ASCs express Oct-4, SOX2, and NANOG

Because ESCs typically express Oct-4, SOX2, and NANOG, which are referred to as pluripotent markers, we wanted to determine the expression levels of these genes in our multipotent ASCs as a means of further classifying them as adult stem cells. We hypothesized that our ASCs would have elevated levels of these pluripotent genes relative to normal, non-multipotent BJ fibroblast cells. In support of this, some studies have indicated increased expression of Oct-4 in ASCs and BM-MSCs after serum deprivation (17). We initially tested our primers using standard, gel-based RT-PCR for visual evidence of Oct-4, SOX2, and/or NANOG, showing that these pluripotent genes are expressed in ASCs from all tissue sources (Figure 3a). Because determining the relative expression levels of genes associated with pluripotency is important for stem cell classification, we also performed qRT-PCR, to determine the quantitative levels of Oct-4, SOX2, and NANOG mRNA transcripts compared to iPS cells (Figure 3b–d). Our baseline expression was set relative to the levels of each transcription factor found in BJ fibroblasts, which express extremely low levels of the respective genes. Both iPS cells, which were created from the same BJ fibroblasts, and cultured ESCs (not shown) served as our positive controls. SOX2 is expressed in ASCs at an average of 10-100-fold higher levels than BJs, while expressing ~10-fold less than the iPS cells (Figure 3b). Oct-4 levels were ~10–100 fold below iPS cells, while significantly higher than BJ fibroblasts (Figure 3c), and NANOG was also measured at 10-100-fold higher levels in ASCs than BJ fibroblasts, while being ~20-fold below iPS cells (Figure 3d). Thus, we found that our ASC cell strains express all three markers of pluripotency at significantly higher levels than both normal BJ fibroblasts and BM-MSCs, independent of the tissue of origin (Figure 3).

### Discussion

Because of damage due to injury or due to the accumulation of changes during the aging process, there is a need to replenish and repair damaged or aged tissues in the human body. As such, multipotent adult human stem cells provide an important source for tissue replenishment in the human body, while also being a critical resource for tissue engineering, whether in the generation of autologous tissues on 3-dimensional matrices or for direct injection into organ sites for repair of damaged tissue. Our purpose for the work presented here is to provide further clarification and classification of the stemness of adipose-derived human adult stromal/stem cells isolated from various fat depots within the human body. We find that our ASCs, independent of the site of isolation, have the capacity to readily differentiate into bone, cartilage, and fat, consistent with the differentiation capacity of mesenchymal stem cells from bone marrow. Of note, all of our tissues were obtained as medical waste, meaning that we are unable to obtain more information that could identify patients. Being unable to collect potential patient identifier data prevents more rigorous comparisons between patients based on metrics such as BMI, diabetic status, race, metabolism, etc. However, we do know that all of our patients are female and ranged in age from 16–60, which is a broad enough variation to claim that age seems to play a negligible role in the ability of these cells to differentiate into mesenchymal cell types. It is also interesting to speculate that because women store and metabolize fat differently than men, variation in differentiation and/or expression of Oct-4/SOX2/NANOG could exist when comparing genders.

Importantly, obtaining ASCs is substantially easier than obtaining BM-MSCs, which is not only a painful aspiration from the iliac crest but also results in a lower yield and a reduced life span compared to our ASCs. Thus, ASCs are a much more accessible and plentiful



source of stem cells that share functional similarities with BM-MSCs. In fact, we have recently identified a population of ASCs (presented here as ASC 12s) that can be readily isolated from the saline fraction of lipoaspirate without the previous lengthy isolation procedure, making them even more easily attainable for stem cell-related studies (18) and differing from previous studies suggesting sonication increases cellular damage and loss of proliferative capacity (29). Overall, our results demonstrate that the ASCs from lipoaspiration of tissues throughout the body remain functionally normal and viable without compromising their stem cell-like features.

We also sought to define a subset of cell surface markers as a means to formally identify ASCs as adult stem cells and to clarify some of the inconsistency in the field. We find no definitive immunophenotype for our ASCs that would distinguish them from either normal fibroblasts or BM-MSCs using a standard, well-accepted subset of surface markers previously thought to be relatively specific for adult stem cells. In addition, our ASCs lack telomerase expression and gradually shorten their telomeres with advancing age, indicating a telomere-based senescence mechanism. While collectively these data suggest that ASCs, in many ways, behave like normal diploid fibroblasts, our results also define ASCs as multipotent with high expression of markers of pluripotency, allowing ASCs to be classified as adult stem cells.

The multipotent differentiation capacity and elevated Oct-2, SOX2, and NANOG expression are consistent with a stem cell phenotype, suggesting the possibility that ASCs exist in fat stores throughout the body as a more primitive cell type. However, the lack of telomerase in our ASCs suggests that if these cells do play a critical role in the continued replacement of lost or damaged tissues, the body's ability to signal and use these cells may be reduced as they undergo age-related senescence. One plausible mechanism for the continued maintenance of their stem cell abilities is likely the repeated cycling in and out of a quiescent state after cell division. By remaining in a non-dividing state within the body, ASCs can preserve their stem cell capacity and react to specific stimuli in response to the need for tissue repair and/or regeneration rather than continuous cell division.

The generation of iPS cells using ASCs from human sources has only recently been accomplished using retroviral-mediated ectopic expression of Oct4, SOX2, Klf4, and c-Myc (30), all of which were silenced in the fully iPS cells and replaced by expression of the endogenous gene. For our purposes, it was of interest that iPS generation using ASCs was more than 200-fold more efficient (0.74%) than iPS cells created from normal, terminally differentiated fibroblasts (range from 0.001–0.002%) (30). While their focus was on both the efficiency and the necessity of feeder layers for iPS induction from ASCs, we contend that because these fat-derived stem cells have elevated levels of the pluripotent genes, Oct4, SOX2, and NANOG, ASCs are more primitive than normal fibroblasts and have a greater potential for becoming pluripotent. While it seems plausible that the variations in pluripotent gene expression would have a direct effect on the plasticity of our ASCs, we are currently conducting the studies that will directly address this question.

One possible therapeutic option for the use of ASCs in tissue engineering may be an *ex vivo* cell replacement approach. We suggest that future therapies could isolate ASCs in a non-invasive manner, expand by addition of exogenous telomerase if necessary, and re-implant cells in damaged areas as needed, similar to what other have proposed (27). Such therapies may lead to cures for many diseases such as osteoporosis, arthritis, and possibly diseases of the brain and nervous system that might include spinal cord injuries and Parkinson's disease. Importantly, these procedures would all be autologous, coming from a patient's own cells, avoiding any graft vs. host disease and circumventing much of the controversy surrounding embryonic stem cells.

In conclusion, the common cell surface markers and telomere/telomerase measurements used to identify ASCs succeed in only identifying them as similar to fibroblasts. Our results indicate that ASCs' stemness should be defined by their ability to differentiate into multiple lineages coupled with their expression of the pluripotent stem cell-related genes Oct-4, SOX2, and NANOG in order to functionally distinguish ASCs as more stem cell-like.

## Acknowledgments

Special thanks to Dr. Stephen Chen and the Department of Surgery for assisting with the procurement of lipoaspirate and abdominoplasty specimens. This study was supported in part by the Department of Pathology (S.E.H. and L.W.E.), the Department of Human and Molecular Genetics (S.E.H.), K01CA105050 (L.W.E.) from the National Cancer Institute, W81XWH-09-1-0500 (L.W.E.) from the Department of Defense Breast Cancer Research Program, and the Jeffress Memorial Trust (L.W.E.). The content is solely the responsibility of the authors and does not necessarily represent the official views of the National Cancer Institute or the National Institutes of Health. Flow Cytometry was supported in part by the Massey Cancer Center core grant, NIH Grant P30 CA16059.

## References

1. Izadpanah R, Trygg C, Patel B, Kriedt C, Dufour J, Gimble JM, Bunnell BA. Biologic properties of mesenchymal stem cells derived from bone marrow and adipose tissue. *J. Cell. Biochem.* 2006; 99:1285–97. [PubMed: 16795045]
2. Zuk PA, Zhu M, Mizuno H, Huang J, Futrell JW, Katz AJ, Benhaim P, Lorenz HP, Hedrick MH. Multilineage cells from human adipose tissue: implications for cell-based therapies. *Tissue Eng.* 2001; 7:211–28. [PubMed: 11304456]
3. Astori G, Vignati F, Bardelli S, Tubio M, Gola M, Albertini V, Bambi F, Scali G, Castelli D, Rasini V, Soldati G, Moccetti T. In vitro and multicolor phenotypic characterization of cell subpopulations identified in fresh human adipose tissue stromal vascular fraction and in the derived mesenchymal stem cells. *J. Transl. Med.* 2007; 5:55. [PubMed: 17974012]
4. Katz AJ, Tholpady A, Tholpady SS, Shang H, Ogle RC. Cell surface and transcriptional characterization of human adipose-derived adherent stromal (hADAS) cells. *Stem Cells.* 2005; 23:412–23. [PubMed: 15749936]
5. Kern S, Eichler H, Stoeve J, Klüter H, Bieback K. Comparative analysis of mesenchymal stem cells from bone marrow, umbilical cord blood, or adipose tissue. *Stem Cells.* 2006; 24:1294–1301. [PubMed: 16410387]
6. Leong DT, Khor WM, Chew FT, Lim TC, Hutmacher DW. Viability and adipogenic potential of human adipose tissue processed cell population obtained from pump-assisted and syringe-assisted liposuction. *J. Dermat. Sci.* 2005; 37:169–76.
7. Lin K, Matsubara Y, Masuda Y, Togashi K, Ohno T, Tamura T, Toyoshima Y, Sugimachi K, Toyoda M, Marc H, Douglas A. Characterization of adipose tissue-derived cells isolated with the Celution system. *Cytotherapy.* 2008; 10:417–26. [PubMed: 18574774]
8. Lin G, Garcia M, Ning H, Banie L, Guo YL, Lue TF, Lin CS. Defining stem and progenitor cells within adipose tissue. *Stem Cells Dev.* 2008; 17:1053–63. [PubMed: 18597617]
9. Noël D, Caton D, Roche S, Bony C, Lehmann S, Casteilla L, Jorgensen C, Cousin B. Cell specific differences between human adipose-derived and mesenchymal-stromal cells despite similar differentiation potentials. *Exp. Cell Res.* 2008; 314:1575–84.
10. Rebelatto CK, Aguiar AM, Moretão MP, Senegaglia AC, Hansen P, Barchiki F, Oliveira J, Martins J, Kuligovski C, Mansur F, Christofis A, Amaral VF, Brofman PS, Goldenberg S, Nakao LS, Correa A. Dissimilar differentiation of mesenchymal stem cells from bone marrow, umbilical cord blood, and adipose tissue. *Exp. Biol. Med. (Maywood).* 2008; 233:901–13. [PubMed: 18445775]
11. Wagner W, Wein F, Seckinger A, Frankhauser M, Wirkner U, Krause U, Blake J, Schwager C, Eckstein V, Anso. Comparative characteristics of mesenchymal stem cells from human bone marrow, adipose tissue, and umbilical cord blood. *Exp. Hematol.* 2005; 33:1402–16. [PubMed: 16263424]

12. Yoshimura K, Shigeura T, Matsumoto D, Sato T, Takaki Y, Aiba-Kojima E, Sato K, Inoue K, Nagase T, Koshima I, Gonda K. Characterization of freshly isolated and cultured cells derived from the fatty and fluid portions of liposuction aspirates. *J. Cell. Phys.* 2006; 208:64–76.
13. Zhu Y, Liu T, Song K, Fan X, Ma X, Cui Z. Adipose-derived stem cell: a better stem cell than BMSC. *Cell Biochem. Funct.* 2008; 26:664–75. [PubMed: 18636461]
14. Torsvik A, Røsland GV, Svendsen A, Molven A, Immervoll H, McCormack E, Lønning PE, Primon M, Sobala E, Tonn JC, Goldbrunner R, Schichor C, Mysliwicz J, Lah TT, Motaln H, Knappskog S, Bjerkvig R. Spontaneous malignant transformation of human mesenchymal stem cells reflects cross-contamination: putting the research field on track. *Cancer Res.* 2010; 70:6393–6. [PubMed: 20631079]
15. Abdallah BM, Haack-Sørensen M, Burns JS, Elsnab B, Jakob F, Hokland P, Kassem M. Maintenance of differentiation potential of human bone marrow mesenchymal stem cells immortalized by human telomerase reverse transcriptase gene despite extensive proliferation. *Biochem. Biophys. Res. Comm.* 2005; 326:527–38. [PubMed: 15596132]
16. Fu WY, Lu YM, Piao YJ. Differentiation and telomerase activity of human mesenchymal stem cells. *Di Yi Jun Yi Da Xue Xue Bao.* 2001; 21:801–805. [PubMed: 12426175]
17. Pochampally RR, Smith JR, Ylostalo J, Prockop DJ. Serum deprivation of human marrow stromal cells (hMSCs) selects for a subpopulation of early progenitor cells with enhanced expression of OCT-4 and other embryonic genes. *Blood.* 2004; 103:1647–52. [PubMed: 14630823]
18. Francis MP, Sachs PC, Elmore LW, Holt SE. Isolating adipose-derived mesenchymal stem cells from lipoaspirate blood and saline fraction. *Organogenesis.* 2010; 6:10–14.
19. Poynter KR, Sachs PC, Breed MS, Bright AT, Nguyen BN, Elmore LW, Holt SE. Genetic inhibition of telomerase: implications for recovery and chemosensitization. *Molec. Cancer Ther.* 2009; 8:1319–1327. [PubMed: 19417141]
20. Elmore LW, Rehder CW, Di M, McChesney PA, Jackson-Cook CK, Gewirtz DA, Holt SE. Adriamycin-induced replicative senescence in tumor cells requires functional p53 and telomere dysfunction. *J. Biol. Chem.* 2002; 277:35509–35515. [PubMed: 12101184]
21. Rooney, D.; Czepulkowski, B. *Human Cytogenetics: A practical approach, Vol II Malignancy and Acquired Abnormalities.* 2nd edition. Oxford University Press; New York: 1992. p. 198-200.
22. Barch, M. *The AGT Cytogenetics Manual.* 3rd Edition. Lippencott Williams and Wilkins; Philadelphia: 1991. p. 263-265.
23. Peng L, Jia Z, Yin X, Zhang X, Liu Y, Chen P, Ma K, Zhou C. Comparative analysis of mesenchymal stem cells from bone marrow, cartilage, and adipose tissue. *Stem Cells Dev.* 2008; 17:761–73. [PubMed: 18393634]
24. Izadpanah R, Kaushal D, Kriedt C, Tsien F, Patel B, Dufour J, Bunnell BA. Long-term in vitro expansion alters the biology of adult mesenchymal stem cells. *Cancer Res.* 2008; 68:4229–38. [PubMed: 18519682]
25. Zimmermann S, Voss M, Kaiser S, Kapp U, Waller CF, Martens UM. Lack of telomerase activity in human mesenchymal stem cells. *Leukemia.* 2003; 17:1146–9. [PubMed: 12764382]
26. Kang SK, Putnam L, Dufour J, Ylostalo J, Jung JS, Bunnell BA. Expression of telomerase extends the lifespan and enhances osteogenic differentiation of adipose tissue-derived stromal cells. *Stem Cells.* 2004; 22:1356–72. [PubMed: 15579653]
27. Kassem M, Abdallah BM, Yu Z, Ditzel N, Burns JS. The use of hTERT-immortalized cells in tissue engineering. *Cytotechnology.* 2004; 45:39–46. [PubMed: 19003242]
28. Zhao YM, Li JY, Lan JP, Lai XY, Luo Y, Sun J, Yu J, Zhu YY, Zeng FF, Zhou Q, Huang H. Cell cycle dependent telomere regulation by telomerase in human bone marrow mesenchymal stem cells. *Biochem. Biophys. Res. Comm.* 2008; 369:1114–9.
29. Oedayrajsingh-Varma MJ, van Ham SM, Knippenberg M, Helder MN, Klein-Nulend J, Schouten TE, Ritt MJ, van Milligen FJ. Adipose tissue-derived mesenchymal stem cell yield and growth characteristics are affected by the tissue-harvesting procedure. *Cytotherapy.* 2006; 8:166–77. [PubMed: 16698690]
30. Sugii S, Kida Y, Kawamura T, Suzuki J, Vassena R, Yin YQ, Lutz MK, Berggren WT, Izpisua Belmonte JC, Evans RM. Human and mouse adipose-derived cells support feeder-independent

induction of pluripotent stem cells. *Proc Natl Acad Sci USA*. 2010; 107:3558–63. [PubMed: 20133714]

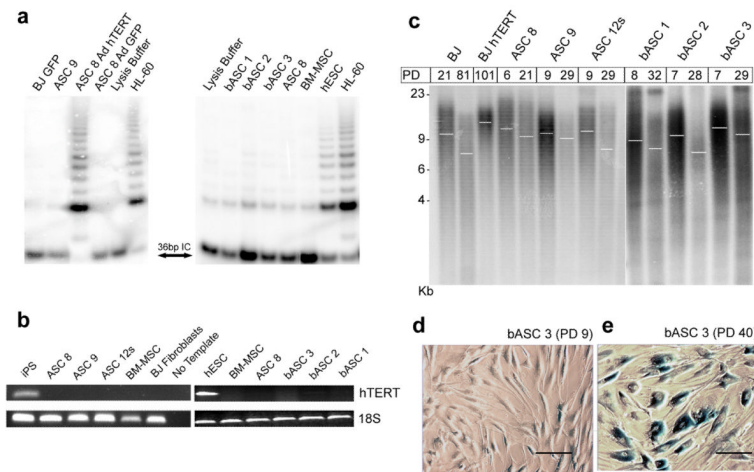


**Figure 1. ASCs lack telomerase activity and exhibit telomere attrition with continued passage**  
**(a)** Telomerase activity was assessed by TRAP for ASC populations isolated from different tissues (bASC denotes breast ASC). Significant activity is shown for Adenoviral hTERT-infected ASC 8. HL-60 and iPS cells served as positive controls. BJ-GFP and a lysis buffer-only samples were used as negative controls. IC denotes 36bp internal control used to standardize sample-to-sample variation. **(b)** Gel-based RT-PCR to detect levels of hTERT in iPS, ASC 8, ASC 9, ASC 12s, ESCs, bASC 1, bASC 2, bASC 3, BM-MSC, and BJ fibroblasts. 18S levels were tested and included as an internal control, while the negative control refers to no template added to the reaction. **(c)** A TRF to examine telomere lengths shows telomere erosion in ASC 8, ASC 9, ASC 12s, bASC 1, bASC 2, and bASC 3 with increased population doubling (PD), as indicated, with BJ fibroblasts at PD 21 and PD 81 as controls for telomere loss. BJ hTERT at PD 101 shows a more uniform telomere length with less heterogeneity for short telomeres. White bars indicate overall mean telomere length. Young bASCs **(d)** versus aged bASCs **(e)** express Senescence-Associated  $\beta$ -galactosidase (SA- $\beta$ -gal) after long-term culture. Representative images for SA- $\beta$ -gal staining are shown for bASC 3 at PD 9 and for bASC 3 after 40 PDs in culture. The scale bar in **(d)** and **(e)** indicates 100 $\mu$ c.

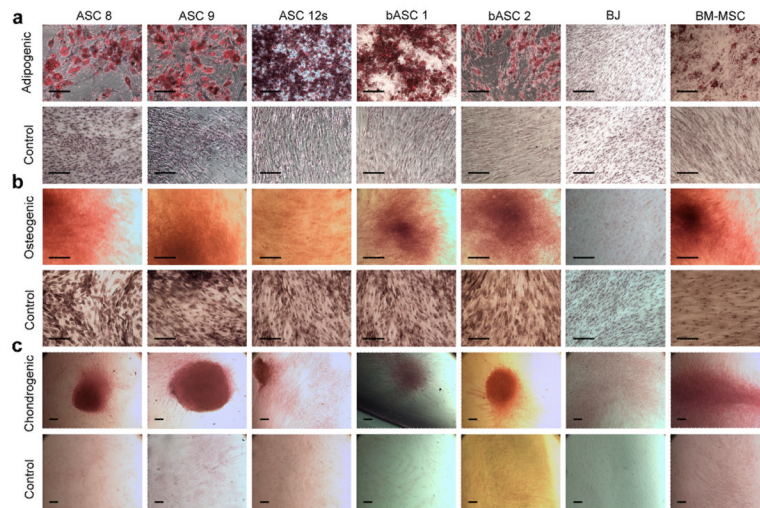


**Figure 2. ASCs differentiate into fat, bone, and cartilage**

ASC 8, ASC 9, ASC 12s, bASC 1, bASC 2, BJ, and BM-MSCs were tested for their ability to differentiate into 3 mesenchymal lineages. Cells grown in control media (standard growth media) served as negative controls. **(a)** Adipogenic differentiation was visualized as lipid droplets in a significant proportion of cells (~70%) after 14 days. Cultures were fixed and stained with Oil Red O to specifically highlight lipid formation indicative of adipocytes. **(b)** All 5 cell strains were incubated at confluency in either osteogenic media or control media for 2–3 weeks to induce osteogenic differentiation. Once cells visually formed aggregates reminiscent of bone nodules and produced significant amounts of calcium deposits (2–3 weeks), cultures were fixed and stained with Alizarin Red S to detect calcium production, which is representative of osteoblast differentiation. **(c)** Following micromass pellet formation (see Experimental Procedures), all cells were continuously cultured in either chondrogenic induction media or control media for 30 days. The entire pellet was processed and stained with Safarin O to permit detection of GAG protein production indicative of chondrogenic differentiation. All images in **(a)** and **(b)** were captured at 10x magnification, while images for **(c)** were captured at 4x magnification. The scale bar in each indicates 100 $\mu$ c.

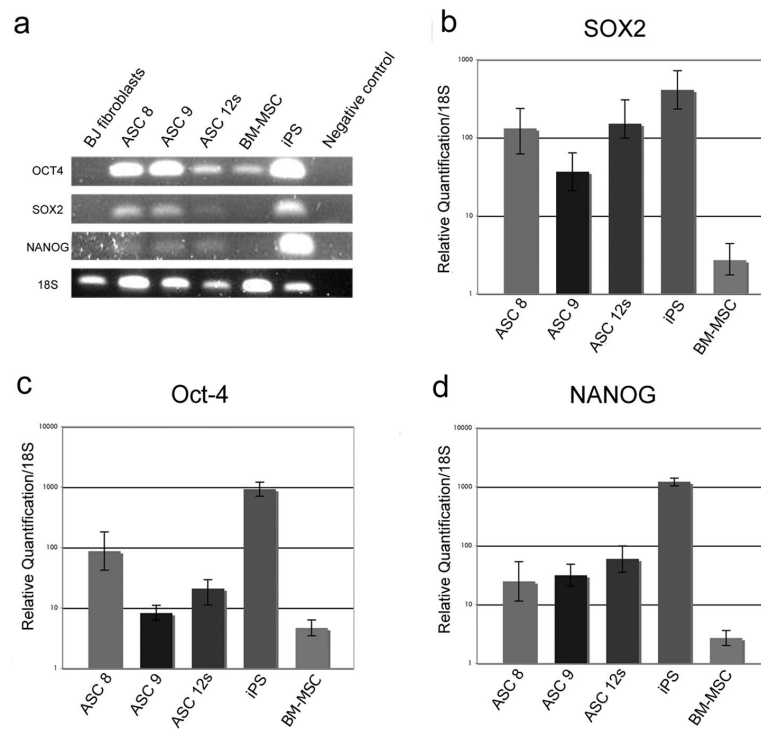


**Figure 3. ASCs express significant levels of pluripotent stem cell markers**

(a) Gel-based RT-PCR for Oct-4, SOX2, NANOG, and 18S compared to controls shows detectable levels of each transcript for each isolated cell strain. (b–d) qRT-PCR of Oct-4, SOX2, and NANOG in ASCs is shown relative to expression in BJ fibroblasts (set as the baseline). Relative expression levels for (b) SOX2, (c) Oct-4, and (d) NANOG were assessed using  $2^{-\Delta\Delta C_t}$  method in ASCs, BM-MSC, and iPS. Data shown are relative to an endogenous control (18S RNA), with fold change compared to expression levels in BJ fibroblasts (set to 1). All lanes shown have a statistical significance of  $p < 0.05$  as compared to BJ fibroblasts using a student's T-test.

**Table 1**

## Growth and Karyotype of ASCs

Cell Strain	Donor Age	PD Time (PD/Day)	PD Max	Karyotype (Metaphases scored)	
ASC 8	33	1.103	48	PD 2	46, XX (8)
				PD21	46, XX (4)
ASC 9	58	0.7443	33	PD13	46, XX (18) inv(9)(p11q13)
				PD20	46, XX (8) inv(9)(p11q13)
ASC 12 s	62	0.5585	27	PD4	46, XX (6)

ASCs – Adipose-derived Stem Cells; PD – population doubling



**Table 2**

## Cell Surface Markers for Cells of Mesenchymal Origin

Cell Type	CD14	CD29	CD31	CD34	CD45	CD73	CD105	References
ASCs	-	+	-	+/-	-	+	+	(Izadpanah et al. 2006; Zuk et al. 2001; Astori et al. 2007; Katz et al. 2005, 2006; Leong et al. 2005; Lin et al. 2008a, b; Noël et al. 2008; Rebelatto et al. 2008; Wagner et al. 2005; Yoshimura et al. 2006; Zhu et al. 2008)
ASCs P0	n.d.	+	-	+	-	n.d.	-	(Wagner et al. 2005)
BM-MSCs	-	+	-	-	-	+	+	(Izadpanah et al. 2006; Zuk et al. 2001; Kern et al. 2006; Lin et al. 2008b; Noël et al. 2008; Rebelatto et al. 2008; Wagner et al. 2005; Zhu et al. 2008)
SVF	n.d.	n.d.	-	+	-	+	+	(Lin et al. 2008b; Wagner et al. 2005)
Umbilical Cord Blood	-	+	-	-	-	+	+	(Kern et al. 2006; Noël et al. 2008; Rebelatto et al. 2008)
Fibroblasts	-	+	-	-	-	+	+	(Kern et al. 2006; Rebelatto et al. 2008; Wagner et al. 2005)
<b>Consensus Profile</b> *	-	+	-	+/-	-	+	+	
ASC – abdomen	-	+	-	+ <sup>low</sup>	-	+	+	N/A
ASC – arms/legs	-	+	-	+ <sup>low</sup>	-	+	+	N/A
ASC – breast (bASC)	-	+	-	+ <sup>low</sup>	-	+	+	N/A
ASC – buttocks	-	+	-	+ <sup>low</sup>	-	+	+	N/A

n.d. – not done; P0 – passage 0, N/A – not applicable

\* average of all data as presence (+), absence (-), or both (+/-);